Preprint Title	Preparation and performance of sensing material for diethyl ether: Optimization of working conditions by response surface methodology
Authors	Wenjuan Zhang, Fuxiu Yang, Hong Wang, Chunxiu Gu, Yun Lu and Kaowen Zhou
Publication Date	30 Mar 2020
Article Type	Full Research Paper
ORCID® iDs	Kaowen Zhou - https://orcid.org/0000-0001-6144-3241

Preparation and performance of sensing material for diethyl ether: Optimization of working conditions by response surface methodology

Wenjuan Zhang[a], Fuxiu Yang[a], Hong Wang[a], Chunxiu Gu[a,b*], Yun Lu[c], Kaowen Zhou[a,b*]

[a]Biochemical Engineering College, Beijing Union University, Beijing 100023, China

[b]Beijing Key Laboratory of Biomass Waste Resource Utilization, Beijing 100023, China

[c]Graduate School of Science and Engineering, Chiba University, Chiba 263-8522, Japan

Abstract

Pd doped $ZnNi_3Al_2O_7$ composite was synthesized by sol-gel and impregnation method. The EDS spectrum and TEM image showed that Pd atoms are uniformly distributed on the surface of $ZnNi_3Al_2O_7$ with a particle size of less than 50 nm. A sensitive diethyl ether gas sensor based on cataluminescence on the composite at lower temperature than 200℃ was reported. There is a good linear relationship between the luminescence intensity and the concentration of diethyl ether in the range of 0.1-75 mg/m^3. The detection limit (3σ) is 0.06 mg/m^3. The working conditions optimized by response surface methodology were analytical wavelength of 548.86 nm, reaction temperature of 109.18℃ and carrier gas velocity of 125.88 ml/min, respectively. The sensitivity of the method can be increased by 4.5% under the optimized working conditions. The optimization method is universal for many multi parameter processes.

Keywords: Diethyl ether; Cataluminescence; Low temperature; Sensitive material; Response surface methodology

*Kaowen Zhou: zhoukaowen@buu.edu.cn
*Chunxiu Gu: 2543774093@qq.com

1. Introduction

Diethyl ether is a colorless and flammable liquid, which is very volatile and can be miscible with ethanol, acetone, benzene and chloroform. The mixture of gaseous diethyl ether and 10 times volume of oxygen can explode violently in case of fire or electric spark [1,2]. Diethyl ether in the air not only has safety problems, but also affects human health. Large concentration of diethyl ether may cause the person in contact with it to be excited, then sleepy, vomit, pale, slow pulse, hypothermia and irregular breath, even life-threatening. Most of the fatal cases involving diethyl ether reported in the second half of the 19th century and the first half of the 20th century were related to anesthesia, as diethyl ether was widely used as an anesthetic in many countries during this period [3]. When people inhale low concentration diethyl ether for a long time, they may have headache, dizziness, tiredness, drowsiness, proteinuria and erythrocytosis. Therefore, it is necessary to determine the content of diethyl ether in air simply and quickly.

Diethyl ether in air is usually determined by gas chromatography with direct injection. Because this method requires a gas chromatograph, it cannot be done on the spot. Gas sensors are especially suitable for on-site, online or remote measurement. Up to now, there are few reports about other sensing technologies of diethyl ether besides cataluminescence (CTL). CTL, a kind of chemiluminescence (CL) emitted from heterogeneous catalytic oxidation reactions on gas-solid interface, has been considered as a promising energy transduction mechanism for fabricating gas sensors [4]. In recent years, a series of CTL sensing applications have been attempted to develop for diethyl ether [5-14] and many other molecules [15-31] at different laboratories. When using the composites to make diethyl ether gas sensor, high working temperature becomes a main obstacle. Generally, sensors need to be as small or even miniaturized as possible in order to be portable, which determines that they must be a small heat capacity system. We know that it is very easy to control the temperature accurately in the laboratory. However, it is very difficult to maintain the high temperature accuracy and stability in a small heat capacity system, which is totally different from the situation in the laboratory equipment. Our previous work has proposed that CTL baseline instability will occur in a small heat capacity system when the working temperature exceeds 200℃ [4]. In the past, most of the working temperature of the CTL method was more than 200℃. So their sensitive materials are not suitable for making CTL gas sensors. Pd doped composites often exhibit low temperature catalytic oxidation activities for many molecules [32-36]. Our team has found that $Pd/ZnNi_3Al_2O_7$ has low-temperature CTL activity for diethyl ether [37]. It may be a good attempt to fabricate gas sensor by using $Pd/ZnNi_3Al_2O_7$ as sensitive material.

In the past, the working conditions of CTL method were simply determined by single factor experiment [4-31]. We know that the premise of single factor experiment is to assume that there is no interaction between various factors. This assumption is beneficial to the completion of the experiment, but its defects are very obvious. So far, there is no research report about the interaction of different factors on CTL signal and about using statistical model to obtain the optimal experimental conditions. Response surface method (RSM) is a statistical

comprehensive test technique [38-41]. It can be used to analyze the regression relationship between test indexes (dependent variables) and multiple test factors (independent variables). It takes the response of the system as a function of many factors, and synthesizes the finite deterministic "trials" into a response surface to simulate the real state surface. In this way, we can use intuitive observation to select the optimal experimental conditions in the experimental design.

In this work, firstly, Pt doped $ZnNi_3Al_2O_7$ was synthesized and characterized. Then, the experimental conditions were optimized by RSM, and the low temperature CTL properties of the composite were studied. Finally, a feasible method was established for determining diethyl ether by utilizing CTL at lower temperature than 200℃.

2. Experimental

2.1. Chemical reagents and apparatus

Zinc acetate, nickel chloride, aluminum nitrate, hydrochloric acid, malic acid, ammonia, palladium chloride and hydrazine hydrate were purchased from Beijing Chemical Regent Co., LTD. (Beijing, China). Various standard gases of ether, formaldehyde, acetaldehyde, ammonia, benzene, ethanol, sulfur dioxide, hydrogen sulfide, carbon monoxide and carbon dioxide in nitrogen were purchased from Beijing Ya-nan Gas Co., LTD. (Beijing, China). Distilled water was used throughout the whole experiment. The micro area composition and particle morphology of the nano-Pd/$ZnNi_3Al_2O_7$ were investigated by scanning electron microscope (SEM, JEOL-IT500) and transmission electron microscopy (TEM, JEOL-2100) respectively. The CTL intensities were recorded by ultraweak luminescence analyzer manufactured at the Biophysics Institute of Chinese Academy of Science (Beijing, China).

2.2. Synthesis of nano- Pd/$ZnNi_3Al_2O_7$

Zinc acetate, nickel chloride and aluminum nitrate were dissolved in dilute hydrochloric acid. The solution is oscillated by ultrasonic to clear. The malic acid was added into the solution in stirring state, and sol was formed by continuously stirring the solution more than 6 h. The pH value of the solution was adjusted to 5.4 with dilute ammonia water. The solution was stirred for 6 hours and aged for 12 hours. Then the gel was prepared by rotating evaporation. After drying and grinding, the gel is placed in a box type resistance furnace. The temperature is increased to 420 ℃ at the rate of 4 ℃/min and maintained the temperature for 5 hours. The composite powder of ZnO, NiO and Al_2O_3 were obtained by natural cooling. Palladium chloride was dissolved in 10% hydrochloric acid aqueous solution, and the composite powder dispersed by ultrasonic wave was added into the solution under stirring.

Then, 25% hydrazine hydrate aqueous solution was continuously dripped into the solution under stirring. The solution was subjected to aging, filtering, washing, drying and calcining at 280℃ in vacuum oven, successively, to finally get nano-Pd/$ZnNi_3Al_2O_7$ that the content of Pd can be adjusted by changing the concentration of palladium chloride.

2.3. Measurement of CTL signals

The loading of nano-Pd/$ZnNi_3Al_2O_7$, the adjustment of working temperature, the introduction of measured gas sample and the recording of CTL signals can refer to our previous work [29-31].

2.4. Experimental design for RSM optimization

According to the single factor experimental results of analysis wavelength, reaction temperature and carrier gas velocity, the Box-Behnken central composite experiment was designed, and the CTL experimental conditions of diethyl ether were optimized by RSM at three factors and three levels.

3. Results and discussion

3.1. Characterization of sensitive materials

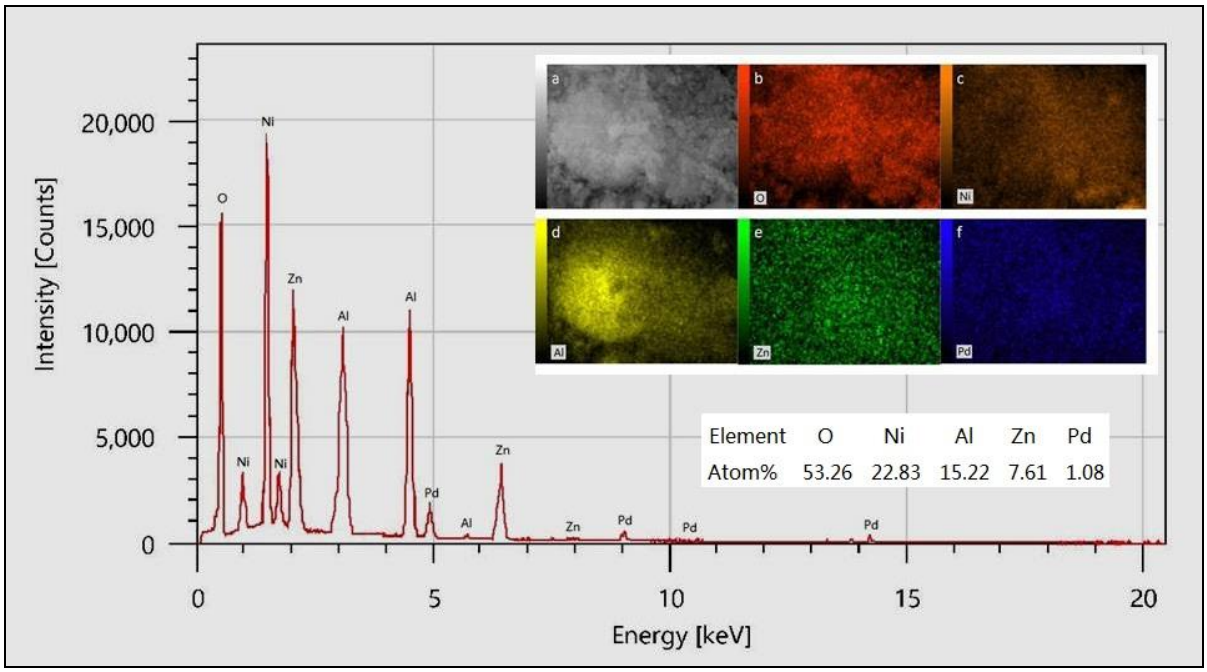

Fig. 1 EDS spectrum of the prepared Pd/$ZnNi_3Al_2O_7$.

The EDS spectrum in Fig. 1 shows that prepared sensitive material is Pd/$ZnNi_3Al_2O_7$, because the atomic ratio of O, Ni, Al and Zn is close to 7:3:2:1. It is found that the content of Pd atom in sensitive materials has a great influence on their CTL activity. When the atomic percentage of Pd is less than 0.8%, the sensitive material has CTL activity to diethyl ether only

when the temperature is above 200 ℃. When the atomic percentage of Pd is more than 1.3%, in addition to diethyl ether, formaldehyde, acetaldehyde, sulfur dioxide, hydrogen sulfide and ammonia also have obvious CTL signals.

The EDS element mapping in the illustration of Figure 1 shows that oxygen, Nickel, aluminum, zinc and palladium were uniformly distributed in the prepared sensitive material. The TEM image in Figure 2a shows that the size of $Pd/ZnNi_3Al_2O_7$ is not more than 50 nm.

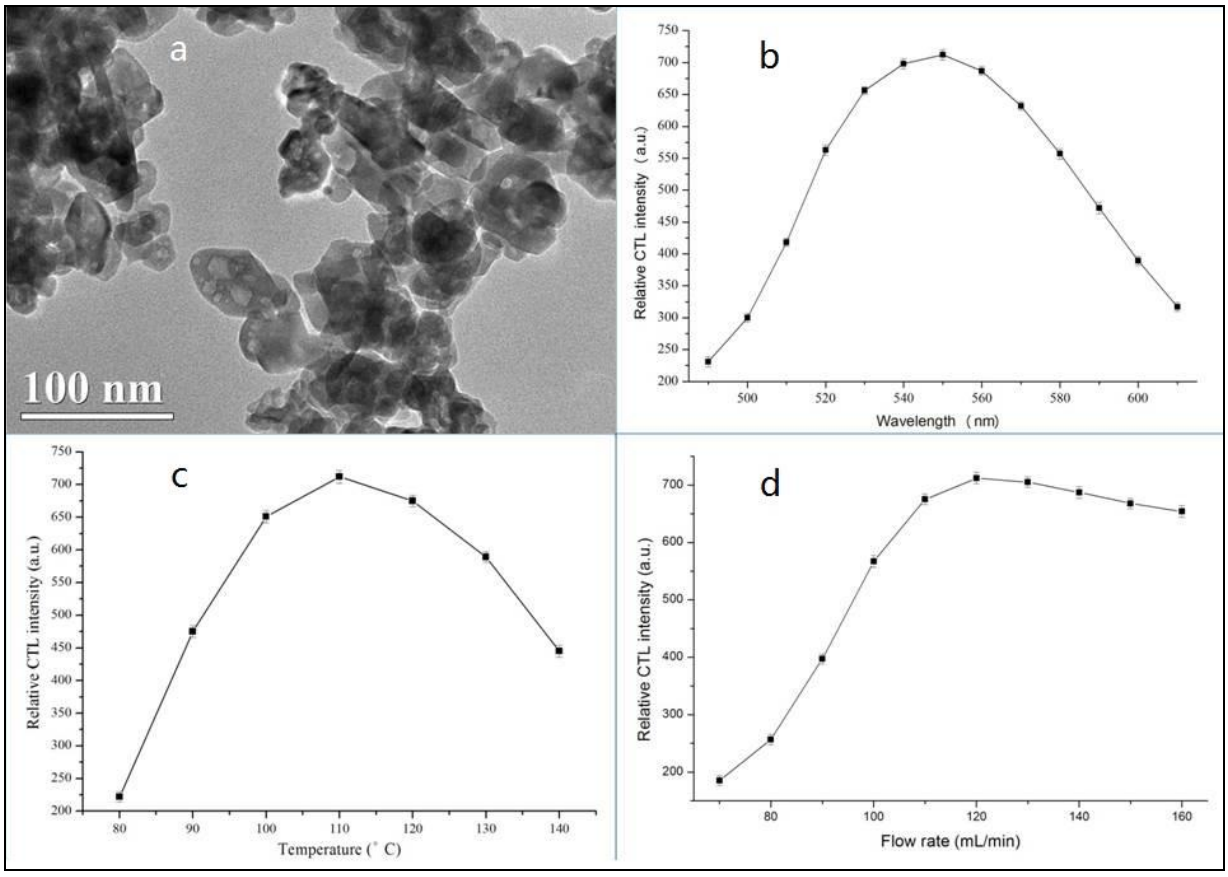

Fig. 2 TEM photo and 3 dependences of CTL intensity.

3.2. Optimization of experimental conditions by single factor test

The effects of analysis wavelength, reaction temperature and carrier gas velocity on the CTL intensity of 5 mg/m^3 diethyl ether on sensitive materials were separately studied.

Fig. 2b is a CTL spectrum of diethyl ether on nano-$Pd/ZnNi_3Al_2O_7$ at 110℃ with a carrier gas velocity of 120ml/min. The CTL intensities were high at 550 nm. Fig. 2c is the temperature dependence of the CTL intensity of diethyl ether at a wavelength of 550 nm under a carrier gas velocity of 120 ml/min. As you can see, the temperature of around 110℃ will be favorable to the determination of diethyl ether. Fig. 2d is the carrier gas velocity dependence of the CTL intensity of diethyl ether at 550 nm and 110℃. The CTL intensity increased with an increase in the carrier gas velocity below 120 ml/min, and it decreased above this velocity.

It can be seen that the operating conditions of simple optimization through single factor experiments are analysis wavelength 550 nm, working temperature 110℃ and carrier gas velocity 120 ml/min.

3.3. Optimization of experimental conditions by RSM

The results of single factor test are summarized. The analysis wavelength, reaction temperature, and carrier gas velocity were used as research factors. The CTL intensity was used as the response value. Three factors and three levels (see table 1) were used to carry out the Box-Behnken test design.

Table 1. Factors and levels of the Box-Behnken test design

Levels\Factors	Wavelength (nm)	Temperature (℃)	Flow rate (mL/min)
-1	540	100	110
0	550	110	120
1	560	120	130

The results of 17 response surface design trials (12 edge points plus 5 center points in Box-Behnken test design) for 5 mg/m^3 diethyl ether are shown in Table 2.

Table 2. Response surface design arrangement and experimental results

Number	Wavelength	Temperature	Flow rate	CTL intensity
1	540.00	120.00	120.00	251
2	550.00	100.00	110.00	311
3	540.00	110.00	110.00	437
4	560.00	110.00	130.00	547
5	550.00	110.00	120.00	712
6	540.00	100.00	120.00	362
7	550.00	110.00	120.00	711
8	550.00	110.00	120.00	713
9	560.00	100.00	120.00	309
10	540.00	110.00	130.00	635
11	550.00	120.00	130.00	394
12	550.00	110.00	120.00	711
13	560.00	120.00	120.00	195
14	550.00	120.00	110.00	237
15	550.00	110.00	120.00	713
16	560.00	110.00	110.00	308
17	550.00	100.00	130.00	467

The 3D surfaces and contours are plotted by Design Expert software, as shown from figure 3 to figure 5. Each figure represents the interaction of two independent variables on the CTL intensity.

Fig. 3 is 3D surface (A) and contours (B) of the effects of analysis wavelength and

reaction temperature on the CTL intensity, respectively. With the increase of the analysis wavelength and reaction temperature, the CTL intensity increases. When the analysis wavelength reaches 548.86 nm and the reaction temperature reaches 109.18 ℃, the CTL intensity reaches its maximum. When the analysis wavelength and reaction temperature continue to increase, the CTL intensity begins to decrease.

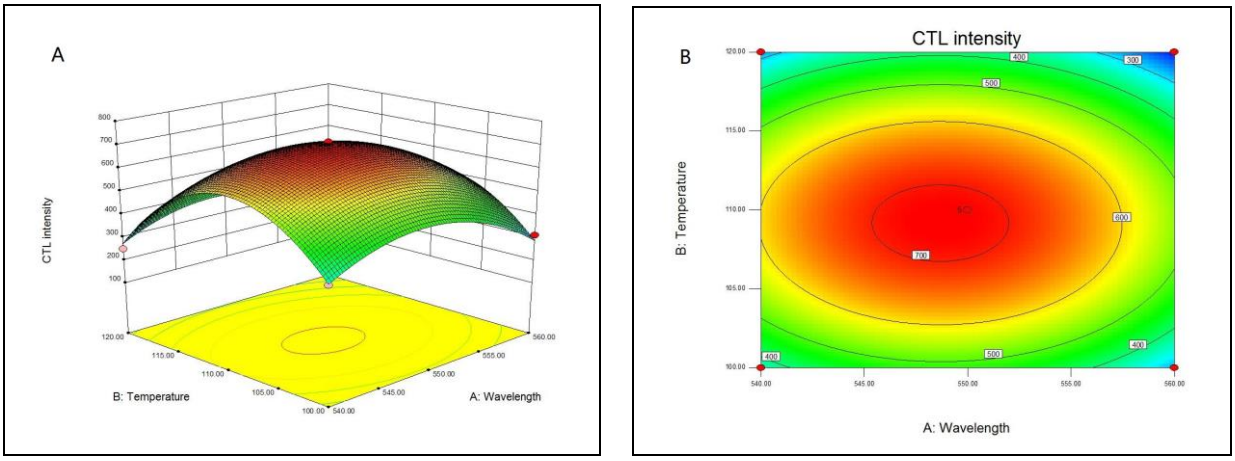

Fig. 3 Response surface and contours of analysis wavelength and reaction temperature.

Fig. 4 is 3D surface (A) and contours (B) of the effects of analysis wavelength and carrier gas velocity on the CTL intensity, respectively. As you can see, when the analytical wavelength reaches 548.86 nm and the carrier gas velocity reaches 125.88 mL/min, the CTL intensity reaches its maximum.

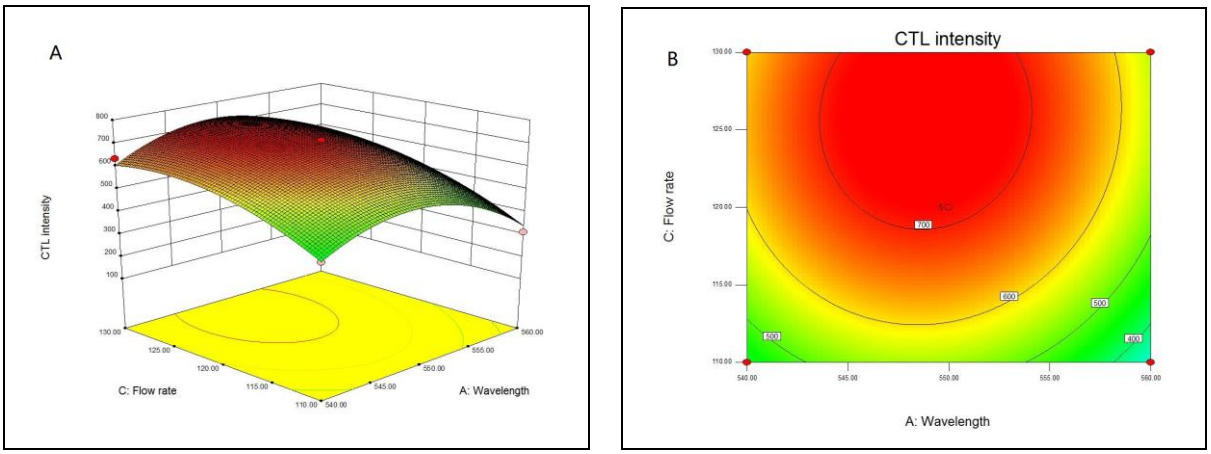

Fig. 4 Response surface and contours of analysis wavelength and carrier gas velocity.

Figure 5 is 3D surface (A) and contours (B) of the effects of reaction temperature and carrier gas velocity on the CTL intensity, respectively. As you can see, when the reaction temperature reaches 109.18 ℃ and the carrier gas velocity reaches 125.88 mL/min, the CTL intensity reaches its maximum.

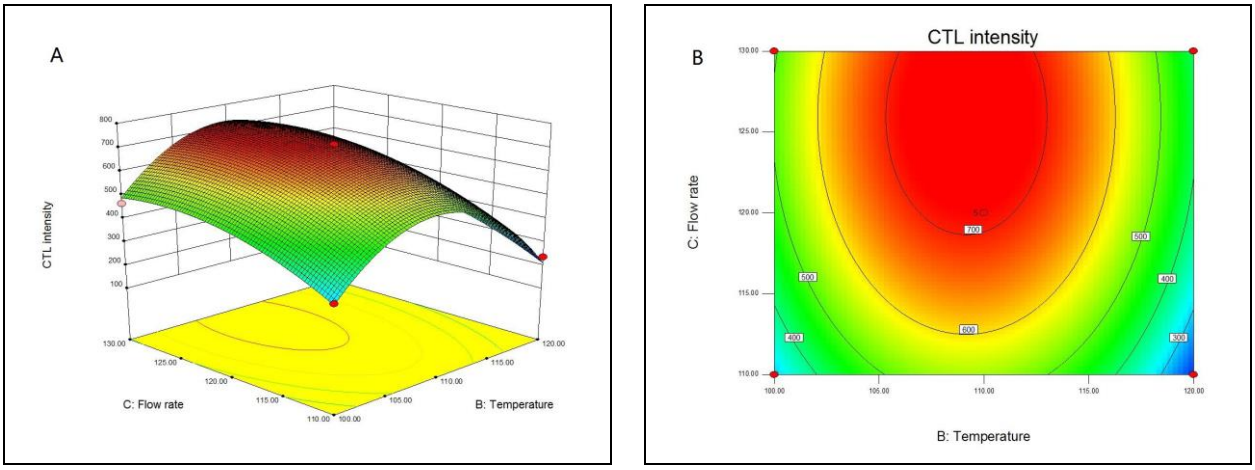

Fig. 5 Response surface and contours of reaction temperature and carrier gas velocity.

Based on the above experimental results, it can be found that the optimum values of analysis wavelength, reaction temperature and carrier gas velocity are 548.86 nm, 109.18 ℃ and 125.88 ml/min, respectively, when the maximum CTL intensity is obtained. It is almost impossible to obtain the optimal operating conditions through single factor experiments, because the number of experiments needed is very large. According to the model, the maximum value of CTL intensity was 744. This is 4.5% higher than the CTL intensity under single factor optimization conditions, which will correspondingly improve the sensitivity of the method.

3.4. Sensing properties

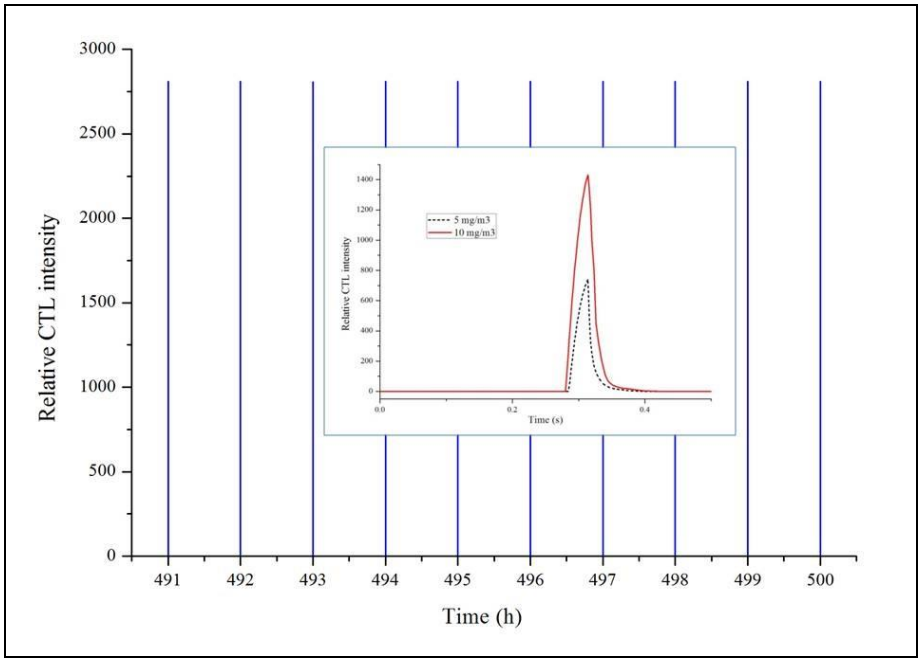

Fig. 6 Response behavior curves of CTL signals and lifetime test.

To investigate the lifetime of the sensitive materials, an experiment was carried out by

continually introducing 20 mg/m^3 diethyl ether in air with the velocity of 125.88 ml/min to the surface of sensitive materials at 109.18°C, and detecting the CTL intensities once every hour at 548.86 nm. Partially recording signals are shown in Fig. 6. The results showed that the relative standard deviation (RSD) of CTL intensities was less than 2.5% for continuous 500 h detection. Further experiments showed that the RSD of the CTL intensities was within 5% for daily use above 10 months. It can be said that nano-Pd/$ZnNi_3Al_2O_7$ has a long service life for diethyl ether monitoring.

Fast signal response is one of the important indicators of sensors. Response characteristics of CTL signals for diethyl ether under the optimization conditions were investigated. Illustration in Fig. 6 signified that there were similar dynamic CTL response curves for diethyl ether at different concentrations. It can be seen that both response and recovery of diethyl ether are singularly fast.

Sulfur dioxide, sulfur dioxide, ammonia, formaldehyde, acetaldehyde, methanol, ethanol, benzene and carbon monoxide are used as interference molecules to study the CTL selectivity of sensitive materials to diethyl ether. The CTL signals of 10 mg/m^3 diethyl ether and 20 mg/m^3 various pollutant molecules in air with the carrier gas velocity of 125.88 ml/min and analysis wavelength of 548.86 nm were investigated on nano- Pd/$ZnNi_3Al_2O_7$ at 109.18℃. The results were shown in Fig. 7.

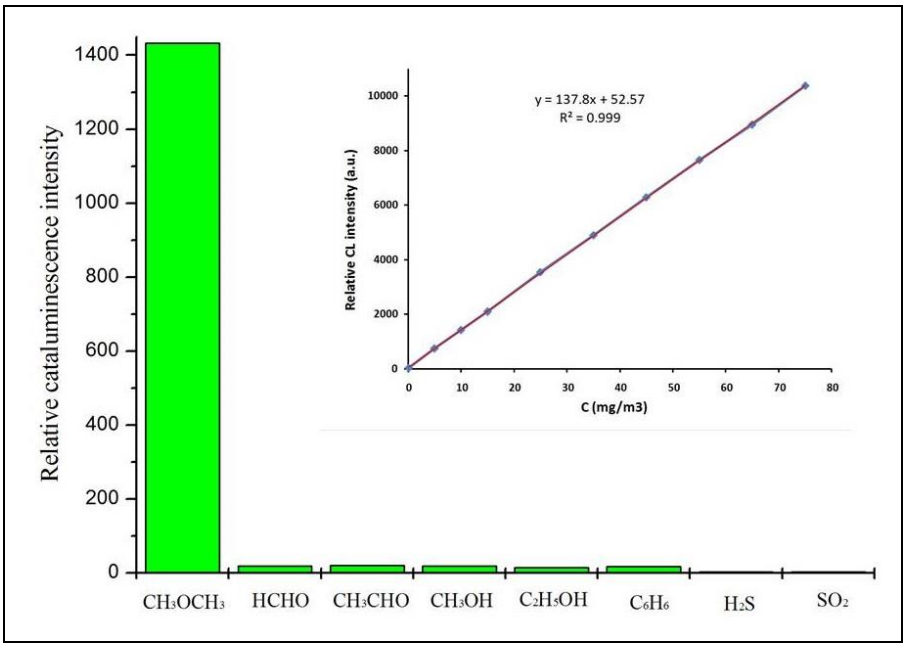

Fig. 7 CTL responses of different gases on nano- Pd/$ZnNi_3Al_2O_7$.

The CTL signals from diethyl ether were much larger than from other molecules. The

signals from formaldehyde, acetaldehyde, methanol, ethanol and benzene were less than 2% of diethyl ether. No visible signals were obtained from hydrogen sulfide, carbon monoxide and sulfur dioxide. It indicated that nano-Pd/$ZnNi_3Al_2O_7$ had good selectivity for diethyl ether under optimization conditions.

Under the optimization conditions, the regression curve of CTL intensity versus diethyl ether concentration was linear in the range 0.1–75 mg/m^3 with a detection limit (3σ) of 0.06 mg/m^3. The linear equation is y = 137.8x+ 52.57 (R^2 = 0.9993) in illustration in Fig. 7, where y is the CTL intensity, x is the concentration of diethyl ether and R is the correlation coefficient.

3.5. Possible luminescence mechanism

We have made a preliminary study on the mechanism of this luminescence reaction. The products of catalytic oxidation were analyzed by GC-MS after molecules in air was introduced. When the surface temperature of catalyst is about 110 ℃, only when there is diethyl ether in the sample gas could the tail gas change, that is to say, a small amount of acetic acid molecule can be detected. There is no change in the other molecules in the sample gas. However, when the catalyst surface temperature is raised to about 160 ℃, except for diethyl ether, both acetic acid and carbon dioxide can be detected. At the same time, many molecules in the sample gas can change at this temperature. For example, a small amount of formaldehyde molecules in the sample gas can be converted into formic acid, few of sulfur dioxide molecules can be converted into sulfur trioxide, trace of acetaldehyde molecules can be converted into acetic acid, etc.

The possible luminescence mechanism is that the active sites produced by the selected catalytic sensitive materials under specific experimental conditions have a good selective adsorption to diethyl ether molecules, and the surface adsorbed oxygen also has a strong reaction activity with it, so diethyl ether is oxidized to acetic acid. The light quantum with ν_1 wavelength can be emitted when the acetic acid molecule on the excited state returns to the ground state. Few acetic acid molecules without leaving the catalyst surface are further oxidized by adsorbed oxygen to carbon dioxide, and the light quantum with ν_2 wavelength can be emitted when the carbon dioxide molecule on the excited state returns to the ground state. The latter reaction is competitive one at high temperature. The reaction mechanism can be expressed by the following formula:

$$CH_3CH_2OCH_2CH_3 + \frac{5}{2}O_2 \rightarrow 2CH_3COOH^* + H_2O$$
$$CH_3COOH^* \rightarrow CH_3COOH + h\nu_1$$
$$CH_3COOH^* + 2O_2 \rightarrow 2CO_2^* + 2H_2O$$
$$CO_2^* \rightarrow CO_2 + h\nu_2$$

4. Conclusions

A sensitive diethyl ether gas sensor based on Pd activated $ZnNi_3Al_2O_7$ at 109.18°C was demonstrated. The detection range is 0.1–75 mg/m^3, and the detection limit is 0.06 mg/m^3. The atomic percentage of 0.8-1.3% Pd in nano-composites was beneficial to low operating temperature and high selectivity for the chemiluminescence of diethyl ether. The sensitivity of the method can be increased by 4.5% after optimizing the experimental conditions by response surface methodology.

Acknowledgements

This work was supported by Beijing Natural Science Foundation (Grant No.2152013), Science and Technology Innovation Project for University Students of Beijing Union University (201911417XJ262) and Postgraduate Funding Project of Beijing Union University (2019-068).

References

[1]C. Bai, N. Liu, B. Zhang, Experimental investigation on the lower flammability limits of diethyl ether/n-pentane/epoxypropane-air mixtures, J. Loss Prevent. Proc., 57(2019) 273-279.

[2]C. Bai, Y. Wang, Study of the explosion parameters of vapor-liquid diethyl ether/air mixtures, J. Loss Prevent. Proc., 38(2015) 139-147.

[3]F. Monticelli, R. Kemmerling, K. Schulz, T. Keller, Another case of diethyl ether intoxication? A case report focusing on toxicological analysis, Legal Med-Tokyo, 13(2011) 254-258.

[4]F. Yang, C. Gu, B. Liu, C. Hou, K. Zhou, Pt-activated Ce4La6O17 nanocomposites for formaldehyde and carbon monoxide sensor at low operating temperature, J. Alloy. Compd, 787(2019) 173-179.

[5]Y. Wang, K. Hu, Y. Zhang, X. Ding, Dendritic fibrous nano-silica & titania (DFNST) spheres as novel cataluminescence sensing materials for the detection of diethyl ether, Rsc Adv, 9(2019) 39622-39630.

[6]Y. Zhen, H. Zhang, F. Fu, Y. Zhang, A cataluminescence sensor based on -MoO3 nanobelts with low working temperature for the detection of diethyl ether, J. Mater. Sci.-Mater. El., 30(2019) 3722-3728.

[7]L. Zhang, N. He, W. Shi, C. Lu, A cataluminescence sensor with fast response to diethyl ether based on layered double oxide nanoparticles, Anal. Bioanal. Chem., 408(2016) 8787-8793.

[8]L. Zhang, S. Wang, Z. Yuan, C. Lu, A controllable selective cataluminescence sensor for diethyl ether using mesoporous TiO2 nanoparticles, Sensor. Actuat. B-Chem., 230(2016) 242-249.

[9]Q. Wang, B. Li, Y. Wang, Z. Shou, G. Shi, Sensitive and selective cataluminescence-based sensor system for acetone and diethyl ether determination, Luminescence, 30(2015) 318-324.

[10]W. Sha, P. Gu, B. Zhang, C. Zheng, A cataluminescence sensor system for diethyl ether based on CdO nanostructure, Meas. Sci. Technol., 25(2014).

[11]J. Chen, X. Cao, R. Xing, L. Xu, Y. Liu, J. Zeng, A sensor system for identifying ether vapors based on extracting two-stage cataluminescence signals, Acta Chim. Sinica, 71(2013) 1421-1428.

[12]J. Liu, Y. Zhang, Y. Yuan, W. Zuo, A Nano-Co3O4-Based low temperature cataluminescence sensor for the detection of gaseous ethyl ether, Acta Chim. Sinica, 71(2013) 102-106.

[13]G. Shi, B. Sun, Z. Jin, J. Liu, M. Li, Synthesis of SiO2/Fe3O4 nanomaterial and its application as cataluminescence gas sensor material for ether, Sensor. Actuat. B-Chem., 171(2012) 699-704.

[14]X. Cao, W. Wu, N. Chen, Y. Peng, Y. Liu, An ether sensor utilizing cataluminescence on nanosized ZnWO4, Sensor. Actuat. B-Chem., 137(2009) 83-87.

[15]K. Yu, J. Hu, X. Li, L. Zhang, Y. Lv, Camellia-like NiO: A novel cataluminescence sensing material for H2S, Sensor. Actuat. B-Chem., 288(2019) 243-250.

[16]G. Shi, Y. He, Y. Zhang, B. Yin, F. Ali, Detection and determination of harmful gases in confined spaces for the Internet of Things based on cataluminescence sensor, Sensor. Actuat. B-Chem., 296(2019).

[17]F. Meng, Z. Lu, R. Zhang, G. Li, Cataluminescence sensor for highly sensitive and selective detection of iso-butanol, Talanta, 194(2019) 910-918.

[18]L. Li, C. Wei, H. Song, Y. Yang, Y. Xue, D. Deng, Y. Lv, Cataluminescence coupled with photoassisted technology: A highly efficient Metal-Free gas sensor for carbon monoxide, Anal. Chem., 91(2019) 13158-13164.

[19]S. Kato, Y. Ito, Y. Ikuta, A. Morikawa, A. Suda, T. Tanabe, Demonstrating the potential of chemiluminescence as a tool to characterize heterogeneous catalysis using CO oxidation on Copper-Based catalysts as an example, 2019.

[20]L. Li, D. Deng, S. Huang, H. Song, K. Xu, L. Zhang, Y. Lv, UV-Assisted cataluminescent sensor for carbon monoxide based on Oxygen-Functionalized g-C3N4 nanomaterials, Anal. Chem., 90(2018) 9598-9605.

[21]F. Han, Y. Yang, J. Han, O. Jin, N. Na, Room-temperature cataluminescence from CO oxidation in a non-thermal plasma-assisted catalysis system, J. Hazard. Mater., 293(2015) 1-6.

[22]J. Han, F. Han, J. Ouyang, L. He, Y. Zhang, N. Na, Low temperature CO sensor based on cataluminescence from plasma-assisted catalytic oxidation on Ag doped alkaline-earth nanomaterials, Nanoscale, 6(2014) 3069-3072.

[23]X. Wu, R. Zong, Y. Zhu, Enhanced MnO2 nanorods to CO and volatile organic compounds oxidative activity by platinum nanoparticles, Acta Phys.-Chim. Sin., 28(2012) 437-444.

[24]N. Zeng, Z. Long, Y. Wang, J. Sun, J. Ouyang, N. Na, An acetone sensor based on Plasma-Assisted cataluminescence and mechanism studies by online ionizations, Anal. Chem., 91(2019) 15763-15768.

[25]R. Zhang, Y. Wang, Z. Zhang, J. Cao, Highly sensitive acetone gas sensor based on g-C3N4 decorated MgFe2O4 porous microspheres composites, Sensors-Basel, 18(2018).

[26]G. Shi, Y. He, Q. Luo, B. Li, C. Zhang, Portable device for acetone detection based on cataluminescence sensor utilizing wireless communication technique, Sensor. Actuat. B-Chem., 257(2018) 451-459.

[27]Y. Weng, D. Deng, L. Zhang, Y. Su, Y. Lv, A cataluminescence gas sensor based on mesoporous Mg-doped SnO2 structures for detection of gaseous acetone, Anal Methods-Uk, 8(2016) 7816-7823.

[28]Z. Li, W. Xi, C. Lu, Hydrotalcite-assisted cataluminescence: A new approach for sensing mesityl oxide in aldol condensation of acetone, Sensor. Actuat. B-Chem., 207(2015) 498-503.

[29]K. Zhou, J. Xu, C. Gu, B. Liu, Z. Peng, Identification and determination of formaldehyde, benzene and ammonia in air based on cross sensitivity of cataluminescence on single catalyst, Sensor. Actuat. B-Chem., 246(2017) 703-709.

[30]K. Zhou, J. Xu, C. Gu, C. Hou, H. Ren, Simultaneous determination of trimethylamine, formaldehyde and benzene via the cataluminescence of In3LaTi2O10 nanoparticles, Microchim. Acta, 184(2017) 2047-2053.

[31]H. Fan, Y. Cheng, C. Gu, K. Zhou, A novel gas sensor of formaldehyde and ammonia based on cross sensitivity of cataluminescence on nano-Ti3SnLa2O11, Sensor. Actuat. B-Chem., 223(2016) 921-926.

[32]X. Du, F. Dong, Z. Tang, J. Zhang, The synthesis of hollow In2O3 @ Pd-Co3O4 core/shell nanofibers with ultra-thin shell for the low-temperature CO oxidation reaction, Appl. Surf. Sci., 505(2020).

[33]Y. He, C. Luan, Y. Fang, X. Feng, X. Peng, G. Yang, N. Tsubaki, Low-temperature direct conversion of methane to methanol over carbon materials supported Pd-Au nanoparticles, Catal. Today, 339(2020) 48-53.

[34]M.D. Marcinkowski, S.F. Yuk, N. Doudin, R.S. Smith, N. Manh-Thuong, B.D. Kay, V. Glezakou, R. Rousseau, Z. Dohnalek, Low-Temperature Oxidation of Methanol to Formaldehyde on a Model Single-Atom Catalyst: Pd Atoms on Fe3O4(001), Acs Catal, 9(2019) 10977-10982.

[35]X. Du, W. Han, Z. Tang, J. Zhang, Controlled synthesis of Pd/CoOx-InOx nanofibers for

low-temperature CO oxidation reaction, New J. Chem., 43(2019) 14872-14882.
[36]A.E.R.S. Khder, H.M. Altass, M.I. Orif, S.S. Ashour, L.S. Almazroai, Preparation and characterization of highly active Pd nanoparticles supported Mn3O4 catalyst for low-temperature CO oxidation, Mater. Res. Bull., 113(2019) 215-222.
[37]K. Zhou, Y. Zhou, W. Li, Y. Zhang, Nanocomposites for monitoring ether, Chinese Patent 201310199379.9, 2015, pp.6.
[38]L. Cristian Favre, G. Rolandelli, N. Mshicileli, L.N. Vhangani, C. Dos Santos Ferreira, J. van Wyk, M. Del Pilar Buera, Antioxidant and anti-glycation potential of green pepper (Piper nigrum): Optimization of beta-cyclodextrin-based extraction by response surface methodology, Food Chem., 316(2020).
[39]M.S. Aragao, D.B. Menezes, L.C. Ramos, H.S. Oliveira, R.N. Bharagava, L.F. Romanholo Ferreira, J.A. Teixeira, D.S. Ruzene, D.P. Silva, Mycoremediation of vinasse by surface response methodology and preliminary studies in air-lift bioreactors, Chemosphere, 244(2020).
[40]P.M. Arruda, E.R. Pereira-Filho, M. Libanio, E. Fagnani, Response surface methodology applied to tropical freshwater treatment, Environ. Technol., 41(2020) 901-911.
[41]K. Dalvand, A. Ghiasvand, Simultaneous analysis of PAHs and BTEX in soil by a needle trap device coupled with GC-FID and using response surface methodology involving Box-Behnken design, Anal. Chim. Acta, 1083(2019) 119-129.